Heat Conduction in Microstructured Materials

Koji Miyazaki, Toyotaka Arashi, Daisuke Makino, and Hiroshi Tsukamoto

***Abstract*—The phonon Boltzmann equation is solved numerically in order to study the phonon thermal conductivity of micro/nanostructured thin films with open holes in a host material. We focused on the size effect of embedded pores and film thickness on the decrease in thermal conductivity of the film. Simulations have revealed that the temperature profiles in the micro/nanostructured materials are very different from those in their bulk counterparts, due to the ballistic nature of the microscale phonon transport. These simulations clearly demonstrate that the conventional Fourier heat conduction equation cannot be applied to study heat conduction in solids at microscale. The effective thermal conductivity of thin films with micro/nanoholes is calculated from the applied temperature difference and the heat flux. In the present paper, the effective thermal conductivity is shown as a function of the size of the micro/nanoholes and the film thickness. For example, when the size of the hole becomes approximately 1/20th the phonon mean free path in a film, the thickness is 1/10th the mean free path of phonons and the effective thermal conductivity decreases to as low as 6% of the bulk value. The distribution of holes also affects the reduction in the effective thermal conductivity. Thin films embedded with staggered-hole arrays have slightly lower effective thermal conductivities than films with aligned-hole arrays. The cross-sectional area in the thermal transport direction is a significant parameter with respect to the reduction of thermal conductivity. The results of the present study may prove useful in the development of artificial micro/nanostructured materials, including thermoelectrics and low-k dielectrics.**

***Index Terms*—Low-k dielectrics, thermoelectrics, thin films.**

NOMENCLATURE

d	Hole size, m.
C	Specific heat per unit volume, $\mathrm{Jm^{-3}K^{-1}}$.
D	Density of states, $\mathrm{m^{-3}s}$.
f	Statistical distribution function.
$\hbar$	Reduced Planck's constant, Js.
I	Directional-spectral phonon intensity, $\mathrm{Wm^{-2}sr^{-1}s}$.
k_{B}	Boltzmann constant, $\mathrm{JK^{-1}}$.
Kn	Knudsen number.
L	Film thickness, m.
p	Interface specularity parameter.
q	Heat flux, $\mathrm{Wm^{-2}}$.
t	Time, s.
T	Temperature, K.
v	Phonon group velocity, $\mathrm{ms^{-1}}$.
x, y, z	Coordinate direction and length, m.

Greek Symbols

δ	Mean free path of phonon, m.
ϕ	Azimuthal angle, rad.
λ	Thermal conductivity, $\mathrm{Wm^{-1}K^{-1}}$.
μ	Directional cosine.
θ	Polar angle, rad.
τ	Relaxation time, s.
ω	Angular frequency of phonons, $\mathrm{s^{-1}}$.
Ω	Solid angle, sr.

Subscripts

B	Bulk.
x	x-direction.
y	y-direction.
ω	Spectral quantity.
0	Equilibrium.

Superscripts

$+$	Forward direction.
$-$	Backward direction.
$*$	Nondimensional.

Manuscript received February 15, 2005; revised February 18, 2006. This work was supported in part by the Japan Society for the Promotion of Science under Grant 16 760 158. This work was recommended for publication by Associate Editor K. Ramakrishna upon evaluation of the reviewers' comments.

K. Miyazaki is with the Department of Biological Functions and Engineering, Kyushu Institute of Technology, Kitakyushu 808-0196, Japan and also with PRESTO, Japan Science and Technology Agency, Kawaguchi City 332-0012, Japan (e-mail: miyazaki@life.kyutech.ac.jp).

T. Arashi is with the Nippon Steel Corporation, Tokyo 100–8071, Japan.

D. Makino is with the Mitsubishi Electric Corporation, Tokyo 100, Japan.

H. Tsukamoto is with the Department of Biological Functions and Engineering, Kyushu Institute of Technology, Kitakyushu 808-0196, Japan.

Digital Object Identifier 10.1109/TCAPT.2006.875905

I. INTRODUCTION

THE thermal conductivity of microstructures is attracting increasing attention due to several important applications of micro/nanostructures, such as the development of efficient thermoelectric materials, porous low-k dielectrics and the thermal management of microelectronic devices and circuits, optoelectronic devices, data storage systems, and microelectromechanical sensors [1]. In dielectrics, heat is transported by phonons, which are quantized lattice waves. Microstructures may reduce thermal conductivity because of the reflection of phonons at interfaces due to acoustic mismatch between the two materials at their interface. Although thermal conductivity reduction is troublesome with respect to the thermal management of semiconductor devices, it can be useful for thermoelectric energy conversion [2]. For example, microstructured materials such as Bi_2Te_3/Sb_2Te_3 superlattices [3] and PbTe/PbSeTe quantum dot superlattices [4] have shown significant enhancement in thermoelectric figure of merit compared to their bulk materials due to their suppressed phonon thermal conductivity. The effective thermal conductivity of composite, or sandwiched, structures has been studied extensively using a variety of methods [5]–[9]. However, the macroscopic models developed using the Fourier heat conduction theory are not valid at microscale due to prevailing ballistic phonon transport at such

length scales [10], [11]. Simulations methodologies and models for phonon transport at microscale are necessary in order to evaluate the effective thermal conductivity of microstructured materials. Atomic simulation approaches such as molecular dynamics [12], [13] and lattice dynamics [14], [15] may have to be employed for this purpose. These methodologies are limited by computational capacity, and are used to study heat conduction in simple planar-layered structures having thicknesses of several nanometers. The Boltzmann transport equation, which describes particle transport in phase space (both spatial and momentum coordinates), appears to be an ideal starting point for the study of heat transfer for nanoscale to macroscale range [10]–[16]. The phonon Boltzmann transport equation has been solved to determine the thermal conductivity of superlattices [17], nanowires [18]–[21] and nanocomposites [22]. Another class of complex microstructured materials, which includes nanoporous materials and nanoporous thin films, may offer high thermoelectric efficiency and has been studied for some time as a class of low-k dielectrics [23], [24]. Few studies have considered the size effect on thermal conductivity, whereby conventional models of the thermal conductivity of porous media break down. In the present study, a two-dimensional (2–D) phonon Boltzmann transport equation [16], [22] has been solved in order to determine the thermal conductivity of thin films with square holes. The effective temperature profiles and effective thermal conductivity of microstructured thin films have been calculated as a function of hole size, arrangement of the holes, and the phonon Knudsen number, which is defined as the phonon mean free path over the thickness of a thin film.

II. Model Development

Heat conduction in semiconductors and dielectric materials mainly occurs by phonon transport. The physics of phonons has been well documented in the literature of conventional solid state physics [25], [26]. In the present study, phonon transport is simulated using the phonon Boltzmann transport equation, which is often used to model the transport of particles such as electrons, dilute gas molecules, phonons and photons [16]

$$\frac{\partial f}{\partial t} + \mathbf{v} \cdot \nabla f = \left(\frac{\partial f}{\partial t}\right)_s \tag{1}$$

where f is the distribution function, which depends on time t, particle position $\mathbf{r}$, and phonon velocity $\mathbf{v}$. For simplicity, the scattering term on the right-hand side of (1) is often approximated by the frequency independent relaxation time [10], [11], [16]–[20], [22]

$$\left(\frac{\partial f}{\partial t}\right)_s = \frac{f_0 - f}{\tau} \tag{2}$$

where f_0 is determined by the Bose–Einstein distribution of phonons and depends on the local equilibrium temperature. In nanostructures, however, local equilibrium cannot be established, and thus the obtained temperature should not be treated as the local equilibrium temperature. Existing theories concerning the frequency dependence of relaxation time contain large uncertainties because they are based on numerous approximations and rely on fitting parameters obtained from experimental data [27], [28]. Therefore, for simplicity, we will use frequency-independent relaxation time approximation.

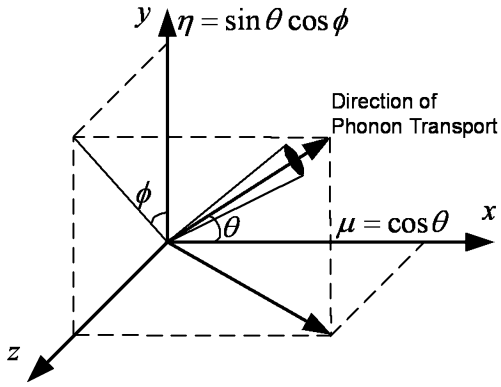

Fig. 1. Schematic diagram of the coordinate system showing the phonon intensity and the various angles of interest.

Phonon number through unit area during unit time multiplied by energy of a single phonon corresponds to energy flow in heat conduction of phonon. Here, energy flow is defined as phonon intensity. In the present study, the direction of energy propagation is described in spherical coordinates, and the phonon intensity is given as

$$I(\theta, \phi, x, y, t) = \frac{1}{4\pi} \sum v f \hbar \omega D(\omega) \tag{3}$$

where θ is the polar angle and ϕ is the azimuthal angle, as shown in Fig. 1. In (3), the phonon intensity is integrated over frequency. We have implicitly assumed that the phonon intensity is independent of frequency. In the present study, only the effects of phonon ballistic transport on heat conduction are included at each position, which simplifies the numerical analysis of the governing equations. Phonon intensity is analogous to photon intensity. Therefore, the techniques used to solve the Boltzmann equation for photons can be applied to the present study. Multiplying (1) by $\mathbf{v}\hbar\omega D(\omega)$ and using the definition of intensity from (3), the following phonon intensity equation is obtained:

$$\frac{1}{v}\frac{\partial I}{\partial t} + \cos\theta\frac{\partial I}{\partial x} + \sin\theta\cos\phi\frac{\partial I}{\partial y} = \frac{I_0[T(x,y)] - I}{v\tau} \tag{4}$$

where the local equilibrium intensity I_0 corresponds to the local equilibrium temperature, which has spatial dependence. When the size of the numerical domain is reduced, the properties should be averaged over a longer time to define local temperature. We have assumed steady-state conditions in the present study because the transient results are artificial in the nanoscopic region

$$I_0[T(x,y)] = \frac{1}{4\pi}\int_0^{2\pi}\int_0^{\pi} I(x,y,\theta,\phi)\sin\theta d\theta d\phi. \tag{5}$$

We have assumed local equilibrium, enabling local definition of temperature, specific heat, and heat flux. The phonon intensity corresponds to the heat flux. The temperature can be calculated by dividing the phonon intensity by the heat capacity. At the atomic scale, the temperature fluctuates with time, and so the effective temperature is calculated by averaging over a long time.

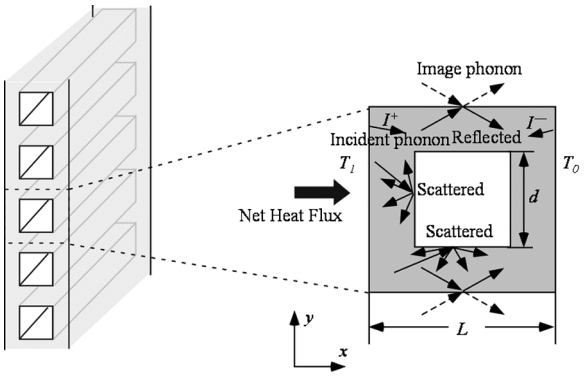

Fig. 2. Schematic diagram of heat transfer in a dielectric microstructured film of thickness L.

Since the steady state is assumed, the effective temperature can be obtained even for a nanoscale solution. The computed temperature should not be treated in the same way as bulk temperature, and it corresponds to a measure of the local energy density. We use the effective temperature to reflect the local energy density inside the medium. Assuming a constant specific heat, the effective temperature is given by

$$T(x,y) = \frac{4\pi I_0(x,y)}{C|v|}. \tag{6}$$

Substituting (5) into (4), we obtain the following equation for the steady state:

$$\cos\theta\frac{\partial I}{\partial x} + \sin\theta\cos\phi\frac{\partial I}{\partial y} = \frac{\frac{1}{4\pi}\int_0^{2\pi}\int_0^{\pi} I(x,y,\theta,\phi)\sin\theta d\theta d\phi - I}{v\tau}. \tag{7}$$

A rigorous phonon transport analysis should take into account the frequency dependence of the phonon relaxation time, group velocity and interactions between phonons. This requires solution of the phonon Boltzmann transport equations over a wide range of frequencies. However, previous research has shown that the average mean free path model of the scattering term is a good approximation for thermal conductivity calculation of the microstructure [10], [11], [16]–[20], [22]. Here, we use the frequency-independent phonon mean free path, $v\tau$, for simplicity. The phonon mean free path is estimated from thermal conductivity, specific heat, and speed of sound, as stated by the standard kinetic theory. The estimated phonon mean free path in Si is on the order of 250 to 300 nm at room temperature [29], [30]. To numerically solve (7), it is convenient to separate the intensity I into a forward component I^+ and a backward component I^-, depending on the direction of the phonon intensity (Refer to Fig. 2). The integral in (7) is approximated by Gaussian–Legender quadrature as

$$\frac{1}{4\pi}\int_0^{2\pi}\int_0^{\pi} I(x,y,\theta,\phi)\sin\theta d\theta d\phi = \frac{2}{4\pi}\sum_m\sum_n I(x,y,\theta,\phi)\sin\theta w_n w_m \tag{8}$$

where w_n and w_m are weighting functions. A value of $\mathrm{N} = 120$ is adequate in the evaluation of the quadrature for each integral. Equation (7) is solved using a finite volume method, and a grid size of 31×31 has been found to be adequate for a relative error of 1×10^{-5} in calculating the phonon intensity between two successive iterations. Effective temperature and heat flux are then calculated using the resulting intensity values. The heat fluxes in the x-direction can be written as

$$q_x(x,y) = \sum_m\sum_n I(x,y,\theta,\phi)\cos\theta w_n w_m. \tag{9}$$

The effective thermal conductivity is calculated using the unit cell concept, in which the average heat flux in the x-direction on the x-plane may be calculated as

$$\bar{q}_x(x) = \frac{1}{L}\int_0^L q_x(x,y)dy. \tag{10}$$

The boundary conditions in the x-direction are

$$I^+ = I_0(T_1) \quad \text{at } x/L = 1.0 \tag{11}$$

$$I^- = I_0(T_0) \quad \text{at } x/L = 0.0 \tag{12}$$

The effective thermal conductivity, λ, of the unit cell is given by

$$\lambda = \frac{\bar{q}_x(0)}{(T_1 - T_0)/L}. \tag{13}$$

The effective temperature distribution is symmetric in the x-direction. When we use $\bar{q}_x(L)$ instead of $\bar{q}_x(0)$ in (13), the same result is obtained.

The use of the isothermal boundary condition in (11) and (12) amounts to using the semi-sphere distribution of phonon intensity. The reflectivity and transmissivity of phonons are not defined at the boundary. The phonon intensity cannot be measured experimentally. For these reasons, the heat conduction in the thin film is computed using the well-known boundary conditions of the phonon intensity. If the structure is not a thin film, other boundary conditions should be considered [22]. In the y-direction, specular reflection of phonons is assumed. Specular reflection of phonons at the boundary conserves phonon momentum and therefore does not impose any resistance to heat transport at the boundary. When the boundary scattering is completely specular, the reflected phonon can be replaced by an image of the incident phonon (see Fig. 2). The film boundaries in the y-direction can essentially be removed and heat transport along the film can be studied as a plane-parallel medium between different temperatures. The following dimensionless parameters have been introduced:

$$x^* = \frac{x}{L}, \quad y^* = \frac{y}{L}, \quad Kn = \frac{\delta}{L}, \quad T^* = \frac{T - T_0}{T_1 - T_0}. \tag{13}$$

The phonon Knudsen number (Kn) is defined as δ/L, where δ is the phonon mean free path and L is the film thickness. Phonon transport becomes ballistic at large phonon Knudsen numbers.

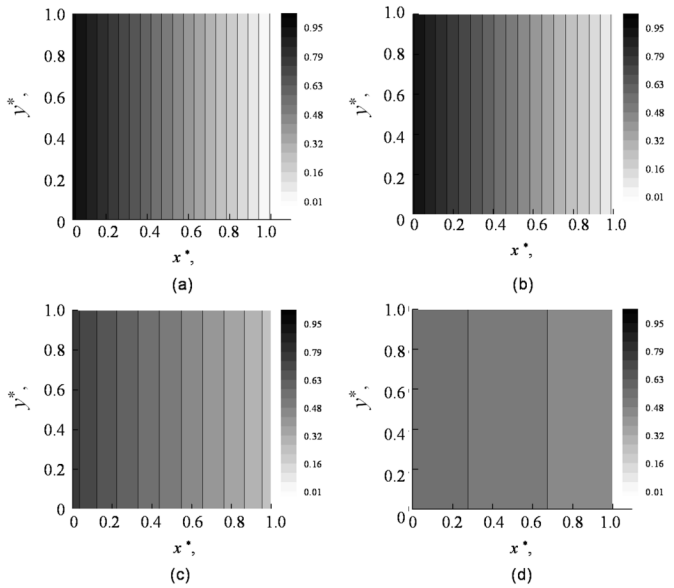

Fig. 3. Nondimensional effective temperature distributions of thin films without structures calculated by solving 2-D Boltzmann equations of phonon transport: (a) Fourier, (b) Kn = 0.1, (c) Kn = 1, and (d) Kn = 10.

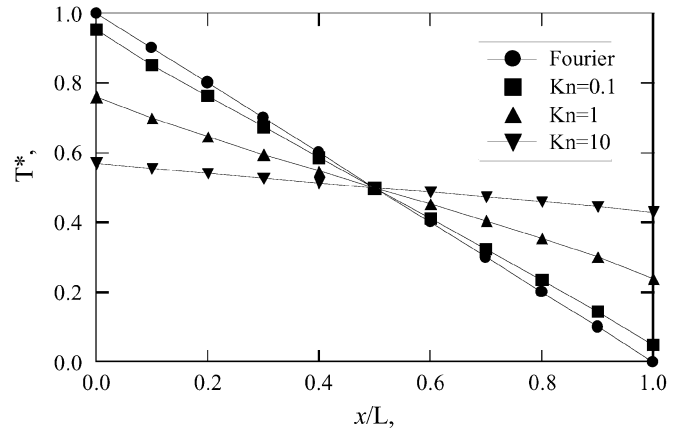

Fig. 4. Non-dimensional effective temperature distribution of thin film in one dimension.

III. Results and Discussions

A. Heat Conduction in Solid Dielectric Thin Film

The validity of the current 2-D model was checked by computing the effective temperature distribution in solid thin film using existing 2-D Boltzmann transport codes. In these simulations, specular reflection is assumed in the y-direction to simulate one-dimensional (1-D) thin films. Specular reflection conserves phonon momentum. Therefore, constant effective temperature distributions in the y-direction are expected in the thin film. The computed isothermal lines are shown in Fig. 3. The effective temperature distributions in Fig. 3 are the same as those obtained for the 1-D calculation, as shown in Fig. 4, which validates the 2-D simulation. When the Kn number is large (i.e., the film is thin compared to phonon mean free path), phonon transport becomes more ballistic, as shown by the small slope of the gradient at $\mathrm{Kn} = 10$ in Fig. 3. In the simulations, the temperature jumps at the boundaries become more significant for a large Kn number. The effective thermal conductivity decreases

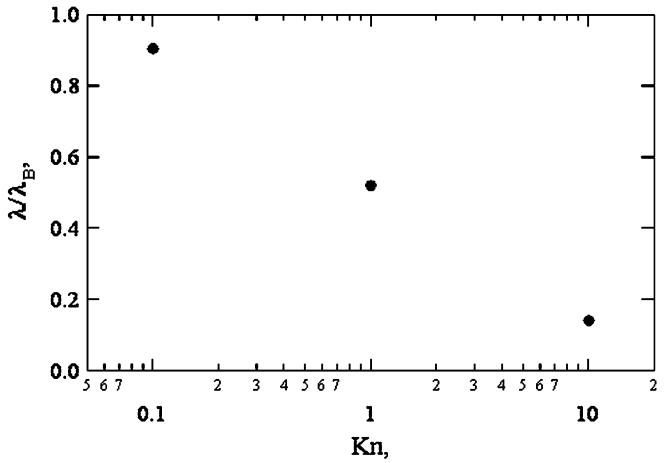

Fig. 5. Effective thermal conductivities of thin films calculated by the gradient of the nondimensional effective temperature at $x^* = 0$.

logarithmically, increasing Kn to approximately 10% of the bulk thermal conductivity at $\mathrm{Kn} = 10$, as shown in Fig. 5. A recent experiment to examine the reduction of the effective cross plane thermal conductivity of SiO_2 thin film shows a similar trend with respect to the decrease in thickness of the thin film [31], [32]. Unfortunately, it is difficult to quantitatively compare the calculated results to the currently available experimental results, because the experimentally measured effective thermal conductivity includes the thermal resistance at the surface or interface. For precise prediction of the thermal conductivity of thin film, a detailed boundary condition with reflectivity and transmissivity should be included in the model. However, the results show the same behavior regarding the thermal conductivity with respect to the thickness of the thin film. The thermal conductivity of the Si thin film has also been measured to be smaller than the bulk value caused by phononinterface scattering [29], [33]. The measured effective thermal conductivity is half of the bulk value. The reduction mechanism of the effective thermal conductivity of thin film in semiconductors and insulators can be explained by this model.

B. Thermal Conductivity of Microstructured Materials

The validated 2-D model given by (7) uses the heat conduction of microstructured materials and microstructured material with a microhole to represent the microstructure. The partially diffuse and partially specular scattering condition has been applied at the interface of these holes. The interface specularity parameter, p, is very important for the reduction of thermal conductivity [17] and should be fitted to experimental data or to molecular dynamics simulation results [34], for example. We used a value of 0.3 for p in the present study, because the interfacial phenomena are too complex to consider herein. Heat conduction in thin films has been investigated for the following range of hole sizes: 0.16L (5/31L), 0.35L (11/31L), and 0.55L (17/31L). The corresponding nondimensional effective temperature profiles of the microstructure are shown in Fig. 6 as gray-scale contour plots. Darker areas represent high-temperature areas, and brighter areas represent low-temperature areas. Thermal energy is transferred from left to right in the figures. When the phonon transport is purely diffusive (i.e., is

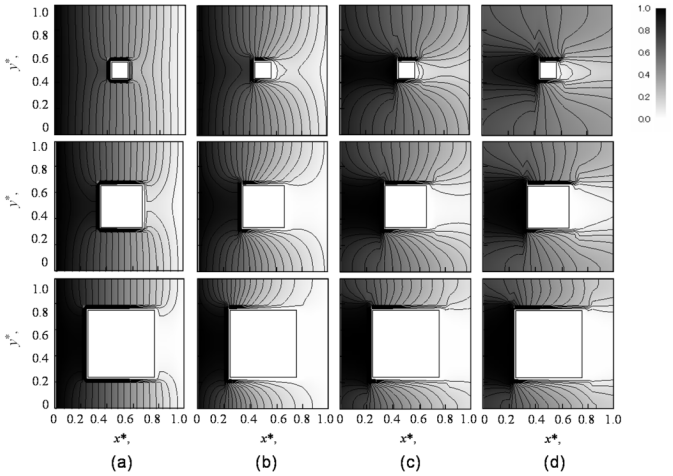

Fig. 6. Nondimensional effective temperature distributions of thin films with a microhole ($p = 0.3$): (a) Fourier, (b) Kn = 0.1, (c) Kn = 1, and (d) Kn = 10.

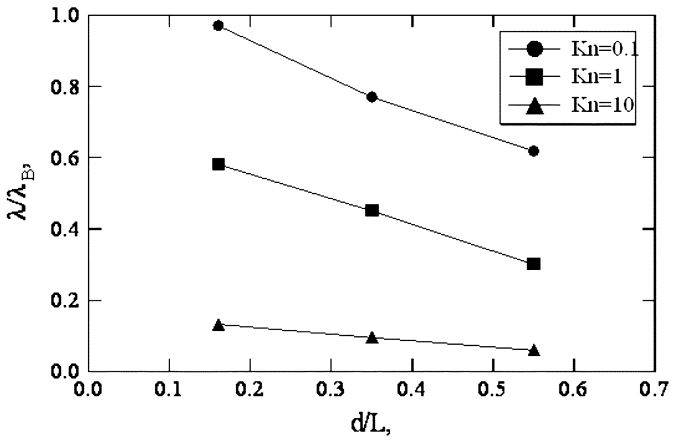

Fig. 7. Effective thermal conductivities of microstructured films under various Knudsen numbers (various film thicknesses).

considered to follow Fourier Law), as shown in Fig. 6(a), the nondimensional effective temperature just behind the hole is 0.33 for the 0.16 L hole. When the phonon transport becomes ballistic, as shown in Fig. 6(b)–(d) at high Kn, ballistic phonons are strongly reflected at the interfaces of the hole. For the 0.16 L hole, the nondimensional effective temperature just behind the hole is less than 0.1 at Kn= 0.1, 1, and 10. As a result of ballistic transport of phonons, a low-temperature area appears behind each hole (as a shadow), as shown in Fig. 6(b)–(d), as is the case in photon transport. The increased low-temperature area indicates a reduction in thermal transport. At high Knudsen numbers, the thermal transport is reduced by the hole, resulting in a reduction of effective thermal conductivity by microstructures such as the microhole. In order to evaluate the effects of the hole on heat transfer, effective thermal conductivities of microstructured materials are calculated. When the hole size becomes approximately 1/20th of mean path of phonons $(\mathrm{Kn} = 10, \mathrm{d/L} = 0.55)$, the effective thermal conductivity decreases to 6% of the bulk value. A two-order of magnitude reduction in thermal conductivity of porous silicon prepared by anodization of silicon wafer, as compared to regular silicon, has been measured experimentally at room temperature [24]. The present computations agree qualitatively with the experimental trends (see Fig. 7).

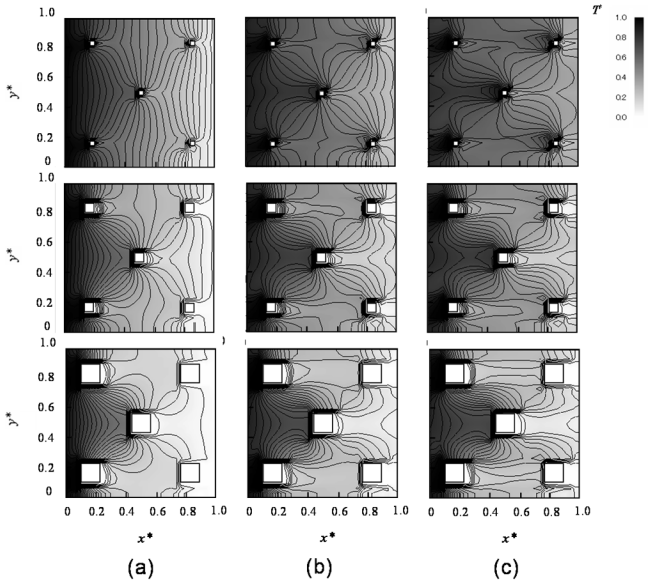

Fig. 8. Nondimensional effective temperature distributions of thin films with staggered microholes ($p = 0.3$): (a) Kn = 0.1, (b) Kn = 1, and (c) Kn = 10.

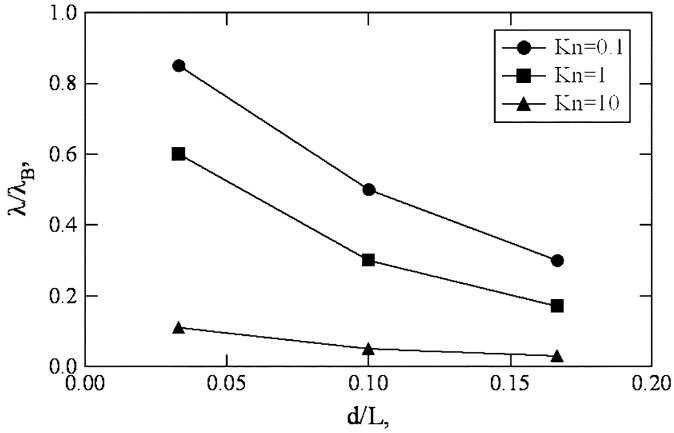

Fig. 9. Effective thermal conductivities of microstructured films with staggered-hole arrays under various Knudsen numbers (various film thicknesses).

C. Thermal Conductivity of Microstructured Materials With Staggered Holes

Numerical analysis shows that ballistic phonons are reflected at the interfaces of micro/nano holes at high phonon Knudsen numbers. When the cross sectional area of holes with respect to the thermal transport direction is increased, heat conduction is suppressed by the reflection of ballistic phonons at the interfaces of the hole, as mentioned in a previous session. In this section, the effects of staggered holes on heat conduction are considered for the following hole sizes: 0.033 L (1/30 L), 0.1 L (3/30 L), and 0.167 L (5/30 L). The total cross-sectional areas of each unit cell are maintained constant and equal to those of the previous simulations for materials with one microhole. The nondimensional effective temperature profiles obtained from these simulations are shown in Fig. 8, and the effective thermal conductivity is shown in Fig. 9. A low-temperature area is computed behind staggered holes as shown in Fig. 8, and thermal transport is found to be reduced by the microstructure. In the previous simulation, periodic microstructures with aligned-hole arrays

are considered because the periodic boundary condition is applied in the y-direction, as shown in Fig. 2. Therefore, the effects of staggered-hole arrays on effective thermal conductivity can be evaluated. Thin films embedded with staggered-hole arrays have slightly lower effective thermal conductivity than thin films with aligned-hole arrays. For example at Kn = 10, the effective thermal conductivity of a thin film with staggered 0.033 L holes is 11% of its bulk value, whereas that of a thin film with a single 0.16 L hole is 13% of its bulk value. The effective thermal conductivities of thin films with 0.033 L, 0.1 L or 0.167 L staggered holes are smaller than those with a single 0.16 L, 0.35 L, or 0.55 L hole, respectively, as shown in Figs. 8 and 9 for Kn= 0.1, 1, and 10. Therefore, the effective thermal conductivity of a thin film with staggered holes is smaller than that of a thin film with aligned holes for holes of the same cross-sectional area. The staggered arrangement of holes may reduce the effective phonon thermal conductivity more than the aligned arrangement of holes.

IV. Conclusion

The 2-D phonon Boltzmann equation was numerically solved in order to calculate the heat transfer in dielectric solid thin films and thin films embedded with aligned or staggered grids of square micro/nanoholes. In addition, a 2-D model validated using existing codes was outlined. The 2-D model was employed to compute temperature profiles in thin films and films with micro/nanosquare holes. The results demonstrate that the effective temperature distributions are very different from those of the conventional heat diffusion equation-based solutions due to the ballistic phonon transport at microscale. When the size of the holes is reduced and/or the Knudsen number is increased (i.e., the film thickness is decreased), ballistic phonon effects become dominant. In such cases, most ballistic phonons are reflected at the hole interfaces, and the heat flux is significantly decreased, which reduces the thermal conductivity. For example, when the size of the hole is on the order of 1/20th of the phonon mean free path of phonons in a thin film with a thickness of only 1/10th of the phonon mean free path, the effective thermal conductivity can be decreased to as low as 6% of its bulk value. We investigated the effects of the arrangement of holes on the effective thermal conductivity. The total cross-sectional area of the holes is a significant parameter that affects the reduction of effective thermal conductivity. In addition, the staggered arrangement of small holes may reduce the effective phonon thermal conductivity further. The simulation results obtained in the present study may prove useful in the development and application of microstructured materials, in which thermal conductivity is an important indicator.

Acknowledgment

The authors would like to thank Dr. G. Chen and Dr. R. Yang, Massachusetts Institute of Technology, Dr. D. Song, Intel Corporation, and Dr. K. Ramakrishna, for their helpful discussions and comments.

References

[1] D. G. Cahill, W. K. Ford, K. E. Goodson, G. D. Mahan, A. Majumdar, H. J. Maris, R. Merlin, and S. R. Phillpot, "Nanoscale thermal transport," *J. Appl. Phys.*, vol. 93, no. 2, pp. 793–818, Jan. 2003.

[2] G. Chen and A. Shakouri, "Heat transfer in nanostructures for solid-state energy conversion," *Trans. ASME J. Heat Transf.*, vol. 124, pp. 242–252, Apr. 2002.

[3] R. Venkatasubramanian, E. Siivola, T. Colpitts, and B. O'Quinn, "Thin-film thermoelectric devices with high room-temperature figures of merit," *Nature*, vol. 413, pp. 597–602, Oct. 2001.

[4] T. C. Harman, P. J. Tayor, M. P. Walsh, and B. E. Laforge, "Quantum dot superlattice thermoelectric materials and devices," *Science*, vol. 297, pp. 2229–2232, Sep. 2002.

[5] J. C. Maxwell, *A Treatise on Electricity and Magnetism*, 3rd ed. London, U.K.: Oxford Univ. Press, 1904.

[6] D. P. H. Hasselman and L. F. Johnson, "Effective thermal conductivity of composites with interfacial thermal barrier resistance," *J. Comp. Mater.*, vol. 21, pp. 508–514, Jun. 1987.

[7] M. Ostoja-Starzewski and J. Schulte, "Bounding of effective thermal conductivities of multiscale materials by essential and natural boundary conditions," *Phys. Rev. B*, vol. 54, pp. 278–285, Jul. 1996.

[8] M. Jiang, I. Jasiuk, and M. Ostoja-Starzewski, "Apparent thermal conductivity of periodic two-dimensional composites," *Computat. Mater. Sci.*, vol. 25, pp. 329–338, Mar. 2002.

[9] S. Graham and D. L. McDowell, "Numerical analysis of the transverse thermal conductivity of composites with imperfect interfaces," *Trans. ASME J. Heat Transf.*, vol. 125, pp. 389–393, Jun. 2003.

[10] A. Majumdar, "Microscale heat conduction in dielectric thin films," *Trans. ASME J. Heat Transf.*, vol. 115, pp. 7–16, Feb. 1993.

[11] A. A. Joshi and A. Majumdar, "Transient ballistic and diffusive phonon heat transport in thin films," *J. Appl. Phys.*, vol. 74, pp. 31–39, Mar. 1993.

[12] S. Volz, J. B. Saulnier, G. Chen, and P. Beauchamp, "Computation of thermal conductivity of Si/Ge superlattices by molecular dynamics techniques," *Microelectron. J.*, vol. 31, no. 9–10, pp. 815–819, Oct. 2000.

[13] B. C. Daly, H. J. Maris, K. Imamura, and S. Tamura, "Molecular dynamics calculation of the thermal conductivity of superlattices," *Phys. Rev. B*, vol. 66, pp. 024 301-1–024 301-7, Jun. 2002.

[14] S. Tamura, Y. Tanaka, and H. J. Maris, "Phonon group velocity and thermal conduction in superlattices," *Phys. Rev. B*, vol. 60, no. 4, pp. 2627–2630, Jul. 1999.

[15] B. Yang and G. Chen, "Partially coherent phonon heat conduction superlattices," *Phys. Rev. B*, vol. 67, pp. 195 311-1–195 311-4, May 2003.

[16] G. Chen, *Nanoscale Energy Transport and Conversion: A Parallel Treatment of Elections, Molecules, Phonons, and Photons*. London, U.K.: Oxford Univ. Press, 2005.

[17] ——, "Thermal conductivity and ballistic-phonon transport in the cross-plane direction of superlattices," *Phys. Rev. B*, vol. 57, no. 23, pp. 14 958–14 973, Jun. 1998.

[18] J. Zou and A. Balandin, "Phonon heat conduction in a semiconductor nanowire," *J. Appl. Phys.*, vol. 89, no. 5, pp. 2932–2938, Mar. 2001.

[19] X. Lu, W. Z. Shen, and J. H. Chu, "Size effect on the thermal conductivity of nanowires," *J. Appl. Phys.*, vol. 91, no. 3, pp. 1542–1552, Feb. 2002.

[20] N. Mingo, "Calculation of Si nanowire thermal conductivity using complete phonon dispersion relations," *Phys. Rev. B*, no. 68, pp. 113 308-1–113 308-4, Sep. 2003.

[21] R. Yang, G. Chen, and M. S. Dresselhaus, "Thermal conductivity of core-shell and tubular nanowires," *Nano Lett.*, vol. 5, no. 6, pp. 1111–1115, Apr. 2005.

[22] R. G. Yang and G. Chen, "Thermal conductivity modeling of periodic two-dimensional nanocomposites," *Phys. Rev. B*, vol. 69, pp. 195 316-1–195 316-10, May 2004.

[23] K. F. Cai, J. P. Liu;, C. W. Nan, and X. M. Min, "Effect of porosity on the thermal-electric properties of Al-doped SiC ceramics," *J. Mater. Sci. Lett.*, vol. 16, no. 22, pp. 1876–1878, Nov. 1997.

[24] A. Yamamoto, H. Takazawa, and T. Ohta, "Thermoelectric transport properties of porous silicon nanostructure," in *Proc. 18th Int. Conf. Thermoelect.*, Baltimore, MD, Aug. 29–Sep. 2 1999, pp. 428–31.

[25] C. Kittel, *Introduction to Solid State Physics*, 6th ed. New York: Wiley, 1986.

[26] N. W. Ashcroft and N. D. Marmin, *Solid State Physics*. Fort Worth, TX: Saunders College, 1976.

[27] S. Mazumder and A. Majumdar, "Monte Carlo study of phonon transport in solid thin films including dispersion and polarization," *Trans. ASME J. Heat Transf.*, vol. 123, pp. 749–759, Aug. 2001.

[28] S. V. J. Narumanchi, J. Y. Murthy, and C. H. Amon, "Submicron heat transport model in silicon accounting for phonon dispersion and polarization," *Trans. ASME J. Heat Transf.*, vol. 126, pp. 946–966, Dec. 2004.
[29] Y. S. Ju and K. E. Goodson, "Phonon scattering in silicon films with thickness of order 100 nm," *Appl. Phys. Lett.*, vol. 74, no. 20, pp. 682–693, Jan. 2004.
[30] C. Dames and G. Chen, "Theoretical phonon thermal conductivity of Si/Ge superlattice nanowires," *J. Appl. Phys.*, vol. 95, pp. 3005–3008, May 1999.
[31] S.-M. Lee and D. G. Cahill, "Heat transport in thin dielectric films," *J. Appl. Phys.*, vol. 81, pp. 2590–2595, Mar. 1997.
[32] B. Popescua, Y. Scudeller, T. Brousse, and B. Garnier, "Thermal characterization of dielectric thin films using an improved genetic algorithm," *Superlatt. Microstruct.*, vol. 35, pp. 239–252, Feb. 2004.
[33] M. Asheghi, K. Kurabayashi, R. Kasnavi, and K. E. Goodson, "Thermal conduction in doped single-crystal silicon films," *J. Appl. Phys.*, vol. 91, no. 8, pp. 5079–5088, Apr. 2002.
[34] P. K. Schelling, S. R. Phillpot, and P. Keblinski, "Phonon wave-packet dynamics at semiconductor interfaces by molecular-dynamics simulation," *Appl. Phys. Lett.*, vol. 80, no. 14, pp. 2484–2486, Apr. 2002.

Koji Miyazaki received the Ph.D. degree from the Tokyo Institute of Technology, Tokyo, Japan, in 1999.

He was a Lecturer in the Department of Mechanical Engineering, Kyushu Institute of Technology, Kitakyushu, Japan, from 1999 to 2000. He was a Visiting Scholar at the University of California, Los Angeles (UCLA), from 2000 to 2001, and at the Massachusetts Institute of Technology, Cambridge, from 2001 to 2002. Currently, he is an Associate Professor in the Department of Biological Functions and Engineering, Kyushu Institute of Technology. His research interests focus on heat transfer at the nanoscopic area.

Toyotaka Arashi received the B.E. degree in mechanical engineering and the M.E. degree in biological functions and engineering from the Kyushu Institute of Technology, Kitakyushu, Japan, in 2003 and 2005, respectively.

He is currently working at Nippon Steel Corporation, Tokyo, Japan. His research interests focus on numerical analysis of heat transfer at the nanoscopic area.

Daisuke Makino received the B.E. and M.E. degrees in mechanical engineering from the Kyushu Institute of Technology, Kitakyushu, Japan, in 2004 and 2006, respectively.

He is currently working at Mitsubishi Electric Corporation, Tokyo, Japan. His research interests focus on numerical analysis of heat transfer at the nanoscopic area.

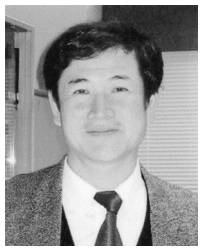

Hiroshi Tsukamoto received the Ph.D. degree from the University of Tokyo, Tokyo, Japan, in 1977.

He was a Lecturer in the Department of Mechanical Engineering, University of Tokyo, from 1977 to 1978, and an Associate Professor from 1978 to 1992, and a Professor from 1992 to 2000 in the Department of Mechanical Engineering, Kyushu Institute of Technology, Kitakyushu, Japan. Since 2000, he has been a Professor of biological functions and engineering at Kyushu Institute of Technology, where he currently serves as Dean of the Graduate School of Life Science and Systems Engineering since 2003. His current research interests include micro and nanofluidics.

Dr. Tsukamoto is a Fellow of The Japan Society of Mechanical Engineers.